

Measuring Top Quark Polarization in Top Pair plus Missing Energy Events

Edmond L. Berger^b, Qing-Hong Cao^a, Jiang-Hao Yu^c, Hao Zhang^{b,d}

^aDepartment of Physics and State Key Laboratory of Nuclear Physics and Technology, Peking University, Beijing 100871, China

^bHigh Energy Physics Division, Argonne National Laboratory, Argonne, IL 60439, USA

^cDepartment of Physics and Astronomy, Michigan State University, East Lansing, MI 48824, USA

^dIllinois Institute of Technology, Chicago, IL 60616-3793, USA

The polarization of a top quark can be sensitive to new physics beyond the standard model. Since the charged lepton from top quark decay is maximally correlated with the top quark spin, it is common to measure the polarization from the distribution in the angle between the charged lepton and the top quark directions. We propose a novel method based on the charged lepton energy fraction and illustrate the method with a detailed simulation of top quark pairs produced in supersymmetric top squark pair production. We show that the lepton energy ratio distribution that we define is very sensitive to the top quark polarization but insensitive to the precise measurement of the top quark energy.

Introduction: Events with a top quark pair plus missing energy ($t\bar{t} + \cancel{E}_T$) are promising channels in which to investigate models of new physics (NP) beyond the standard model (SM). Missing energy originates typically from non-interacting or otherwise invisible dark matter (DM) candidates in the NP models, along with neutrinos from SM decays. In these events the polarization of the top quark is sensitive to the chirality structure of the top quark's interaction with a postulated parent new heavy resonance and the DM. The top quark polarization might provide a new way to gain insight into NP models. Measurements of the top quark polarization tend to rely on the predicted angular correlation of the momentum of a charged lepton (from the top quark decay) with the top quark spin [1]. However, this measurement is difficult in $t\bar{t} + \cancel{E}_T$ events because it is generally not possible to reconstruct the top quark kinematics, i.e., to disentangle the kinematic effects of the DM particles from neutrinos that accompany the charged leptons in the top quark leptonic decay.

In this Letter we define and examine the energy fraction of the charged lepton from the top quark as a novel measure of top quark polarization, without the requirement of top quark reconstruction and knowledge of the dark matter mass and spin. We emphasize a few advantages of our energy ratio variable: (i) it is sensitive to the top-quark polarization; (ii) it is not sensitive to the mass splitting between a heavy resonance parent and the DM candidate, provided that this splitting is not too small; (iii) the difference between the left-handed top-quark (t_L) and the right-handed (t_R) is not sensitive to the spin of a heavy parent resonance or to the collider energy.

We illustrate our method with top squark (\tilde{t}) pair production in the minimal supersymmetric extension of the SM (MSSM), $pp \rightarrow \tilde{t}\tilde{t}X \rightarrow t\tilde{t}\tilde{\chi}\tilde{\chi}X$, where $\tilde{\chi}$ denotes a neutralino (the DM candidate). Once a signal for a \tilde{t} or another such NP candidate has been established, an important next step would be to determine the characteristics of its interaction with the SM particles. We do a full model simulation of $pp \rightarrow \tilde{t}\tilde{t}X \rightarrow t\tilde{t}\tilde{\chi}\tilde{\chi}X$ at the

Large Hadron Collider energy 8 TeV, including typical experimental selection cuts [2]. From these events, we compute the energy fraction of the charged lepton from the top quark decays, show explicitly the relationship of this energy fraction to the top quark spin, and demonstrate what one may conclude about the nature of the interaction of the top quark and top squark from such data. In the MSSM, the t -polarization probes the \tilde{t} - $\tilde{\chi}$ interaction and in turn the top squark mixing [3].

The method: In the leptonic decay of a top quark, $t \rightarrow bW^+ \rightarrow b\ell^+\nu$, the correlation of the momentum of the charged lepton ℓ^+ with the polarization \hat{s}_t of the top quark, viewed in the top quark rest frame, takes the form $(1 + \hat{s}_t z)/2$, where $z \equiv \cos\theta$ is the cosine of the angle between the top quark spin axis and the lepton momentum. For a boosted top-quark with energy E_t , the distribution in the energy fraction $x_\ell \equiv 2E_\ell/E_t$ of the charged lepton becomes

$$\frac{d\Gamma(\hat{s}_t)}{dx} = \frac{\alpha_W^2 m_t}{64\pi AB} \int_{z_{\min}}^{z_{\max}} x\gamma^2 [1 - x\gamma^2(1 - z\beta)] \left(1 + \hat{s}_t \frac{z - \beta}{1 - z\beta}\right) \text{Arctan}\left[\frac{Ax\gamma^2(1 - z\beta)}{B - x\gamma^2(1 - z\beta)}\right] dz. \quad (1)$$

Here, $A = \Gamma_W/m_W$ is the ratio of the W -boson width and W -boson mass, $B = m_W^2/m_t^2 \approx 0.216$ is the ratio of the W -boson mass and top quark mass, and the limits of integration are $z_{\min} = \max[(1 - 1/\gamma^2 x)/\beta, -1]$, $z_{\max} = \min[(1 - B/\gamma^2 x)/\beta, 1]$ with $\gamma = E_t/m_t$ and $\beta = \sqrt{1 - 1/\gamma^2}$. The function Arctan is defined as $\arctan(x)$ for $x \geq 0$ while $\pi + \arctan(x)$ for $x < 0$.

Figure 1(a) displays the normalized energy fraction of the charged lepton from Eq. 1 for three top quark energies, $E_t = (250, 500, 1000)$ GeV, for both left-handed and right-handed top quark decay. The important point [4, 5] is that right-handed top-quarks t_R (dashed curves) produce more energetic leptons than left-handed top-quarks t_L (solid curves), with the difference becoming more pronounced with increasing E_t .

We exploit the different dependence of t_L and t_R on

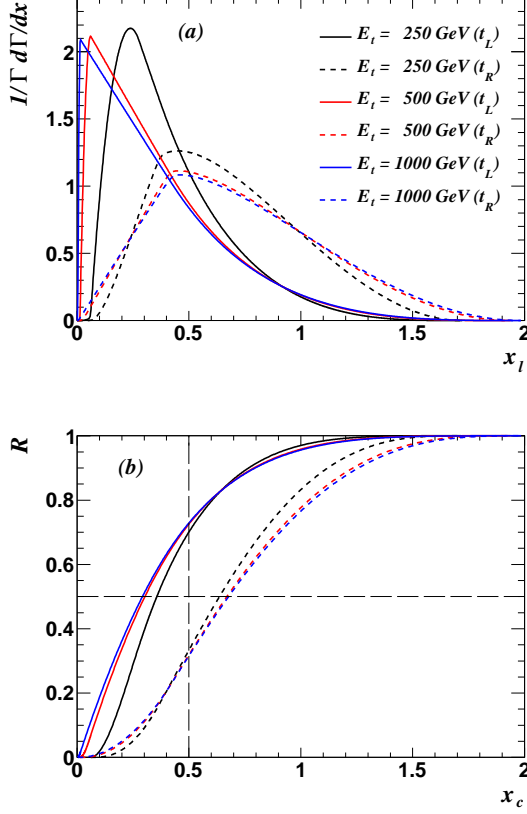


FIG. 1: (a) Distributions of the energy fraction x_ℓ of a charged lepton from top quark decay for $E_t = 250, 500, 1000$ GeV; (b) The ratio \mathcal{R} as a function of the cut threshold x_c for $E_t = 250, 500, 1000$ GeV. The solid lines represent left-handed top quark decay while the dashed lines represent right-handed top quarks.

x_ℓ shown in Fig 1(a) to measure the top quark polarization [6]. We introduce a ratio \mathcal{R} as a quantitative measure of the energy fractions of t_L and t_R ,

$$\mathcal{R}(x_c) = \frac{1}{\Gamma} \int_0^{x_c} \frac{d\Gamma}{dx_\ell} dx_\ell \equiv \frac{\Gamma(x_\ell < x_c)}{\Gamma}. \quad (2)$$

This ratio is a function of the the cut threshold x_c of the energy fraction x_ℓ . We plot the $\mathcal{R}(x_c)$ distribution in Fig. 1(b) for three top quark energies, $E_t = (250, 500, 1000)$ GeV, for both t_L (solid curves) and t_R (dashed curves). While the energy distribution Fig. 1(a) varies with the top-quark energy, the $\mathcal{R}(x_c)$ distribution in Fig. 1(b) shows much less dependence.

An analytic expression can be derived for $\mathcal{R}(x_c)$ in the limit $\beta \rightarrow 1$. It takes the form

$$\mathcal{R}(x_c) = \frac{3x_c(1 - \lambda_t)}{2(1 + 2B)} - \frac{3\lambda_t x_c^2(1 - B + \ln B)}{2(1 + 2B)(1 - B)^2}, \quad (3)$$

for $x_c \in (0, 2B)$, and

$$\mathcal{R}(x_c) = \frac{B^2(2B - 3)}{(1 + 2B)(1 - B)^2} + \frac{3x_c(1 - \lambda_t)}{2(1 - B)^2(1 + 2B)} - \frac{3x_c^2[1 + 2\lambda_t \ln(x_c/2)]}{4(1 - B)^2(1 + 2B)} + \frac{x_c^3(1 + 3\lambda_t)}{8(1 - B)^2(1 + 2B)} \quad (4)$$

for $x_c \in (2B, 2)$, where $\lambda_t = (-1, +1)$ for (t_L, t_R) , respectively. For small x_c , these expressions show that $\mathcal{R}(x_c)$ grows linearly with x_c for t_L , whereas $\mathcal{R}(x_c)$ grows as x_c^2 for t_R ($\lambda_t = 1$).

The analytic expressions Eqs. 3 and 4 also explain why the curves for $E_t = 500$ GeV ($\beta = 0.94$) and $E_t = 1000$ GeV ($\beta = 0.99$) almost overlap. For an energetic top-quark, an important consequence is that the difference between $\mathcal{R}(x_c)$ for t_L and t_R is not sensitive to E_t , i. e., the mass splitting between the parent heavy resonance and the DM candidate, as long as the mass splitting is not too small. The t_L and t_R curves are insensitive to the origin of the top quark in the collision, whether from a heavy fermion decay or from a scalar decay. In other words, $\mathcal{R}(x_c)$ quantifies the top quark polarization but not the top quark origin. Moreover, in order to extract NP signal events from SM backgrounds, one must normally impose a set of hard kinematic cuts on the leptons and jets in the final state. These hard cuts force the top quark to be very energetic and thus to satisfy the limit $\beta \rightarrow 1$. Therefore, another virtue of the $\mathcal{R}(x_c)$ variable is that the difference between t_L and t_R curves, do not vary with the hard cuts.

The ratio $\mathcal{R}(x_c)$ appears to show great promise for distinguishing t_L and t_R . However, even if it is insensitive to E_t , it presupposes reconstruction of the kinematics of the top quark (i.e., knowledge of E_t). Moreover, until this point, we have not included the influence of the production dynamics of the top quark, including matrix elements and the convolution with parton distribution functions. To prove our method useful, we must show that there are good estimators that can replace E_t . To this end, we turn to an explicit calculation of top squark (\tilde{t}) pair production, $pp \rightarrow \tilde{t}\tilde{t}^* \rightarrow t\tilde{\chi}\tilde{\chi}X$.

Collider simulation: We perform a parton-level Monte Carlo simulation of top squark (\tilde{t}) pair production $pp \rightarrow \tilde{t}\tilde{t}^* \rightarrow t\tilde{\chi}\tilde{\chi}X$ to demonstrate that \mathcal{R} remains useful for distinguishing t_L and t_R even when E_t cannot be measured directly. We assume the colored scalar \tilde{t} decays entirely into $t\tilde{\chi}$ through the effective coupling

$$\mathcal{L}_{\tilde{t}\tilde{\chi}} = g_{\text{eff}} \tilde{t}\tilde{\chi}(\cos \theta_{\text{eff}} P_L + \sin \theta_{\text{eff}} P_R)t, \quad (5)$$

where the angle θ_{eff} depends on the mass matrix mixings of the top squark and the neutralino sectors, and $P_{L/R}$ is the usual left/right-handed projector. Our benchmark point has $m_{\tilde{t}} = 360$ GeV and a representative DM mass $m_{\tilde{\chi}} = 50$ GeV. We simulate \tilde{t} pair production with decay to a top quark pair plus dark matter candidates

at the LHC with 8 TeV energy. We demand that the top quark decays semi-leptonically, and that the anti-top quark decays hadronically, $\bar{t} \rightarrow 3\text{jets}$. The final state contains a lepton plus jets and large missing transverse energy \cancel{E}_T . Two irreducible SM backgrounds, $t\bar{t}$ and $t\bar{t}Z$ production, are considered. Both the signal and background processes are generated at leading order in MadGraph/MadEvent [7] with CTEQ6L1 parton distribution functions [8]. The renormalization and factorization scales are chosen as $m_{\tilde{t}}$. Momentum smearing effects are included through a Gaussian-type energy resolution. We apply a set of basic acceptance cuts for the jets and single lepton in the final state: $p_T(\ell) > 20$ GeV, $p_T(j) > 25$ GeV, $|\eta_{\ell,j}| < 2.5$, $\Delta R_{jj,\ell j} > 0.4$, $\cancel{E}_T > 25$ GeV. To suppress SM backgrounds, we impose a set of much harder cuts: $p_T(j_{1st}) > 50$ GeV, $p_T(j_{2nd}) > 40$ GeV, $\cancel{E}_T > 100$ GeV, $H_T > 500$ GeV, where H_T is the scalar sum of the transverse energies of all objects in the event. After the hard cuts, the cut efficiency for the signal is about 44% compared to the rate after the basic cuts. The $t\bar{t}$ background still dominates after the hard cuts, and the $t\bar{t}Z$ background is negligible. In order to further suppress the SM background, we use the fact that \cancel{E}_T originates from the neutralino and neutrino in the signal events while from only the neutrino in the $t\bar{t}$ background. Hence, the neutrino longitudinal momentum $p_{\nu L}$ obtained from the W -boson on-shell condition $m_{\nu}^2 = m_W^2$,

$$p_{\nu L} = \frac{1}{2p_{eT}^2} \left(A p_{eL} \pm E_e \sqrt{A^2 - 4p_{eT}^2 \cancel{E}_T^2} \right), \quad (6)$$

is unphysical more often in the signal than in the background [9]. Here $A = m_W^2 + 2\vec{p}_{eT} \cdot \vec{\cancel{E}}_T$. We then demand $A^2 - 4p_{eT}^2 \cancel{E}_T^2 \leq 0$. We also impose a cut on the transverse mass of the charged lepton and missing energy, $M_T = \sqrt{2p_T^\ell \cancel{E}_T (1 - \cos \phi)} \geq 100$ GeV, where p_T is the lepton transverse momentum and ϕ is the angle in the transverse plane between \vec{p}_T and $\vec{\cancel{E}}_T$. Only about 0.00556% of the $t\bar{t}$ events remain after all the cuts. The cross sections for the signal and main backgrounds are shown in Table I after branching fractions are included. Using these cross sections, we find that the numbers of signal and background events are 130 and 22 at 8 TeV and 20 fb^{-1} integrated luminosity, for a signal significance of $S/\sqrt{B} = 28$.

In \tilde{t} pair production the decay chains of $\tilde{t} \rightarrow t\tilde{\chi}$ and $\bar{\tilde{t}} \rightarrow \bar{t}\tilde{\chi}$ have similar kinematics because the heavy \tilde{t} 's are not highly boosted. In this work we investigate the energy of the anti top-quark as an estimator of the top quark energy, with the anti-top quark required to decay into three jets [13]. We define a new energy fraction variable x'_ℓ ,

$$x'_\ell = 2E_\ell/E_{\bar{t}}. \quad (7)$$

After convolution with the production cross section, a

TABLE I: Cross sections (in fb) for the signal and background processes at different cut levels, including the decay branching fractions to the specific final states of interest.

	<i>Basic</i>	<i>t_{had} recon.</i>	<i>Hard</i>	<i>\cancel{E}_T sol.</i>	ϵ_{cut}
signal	22.26	18.46	8.87	6.51	11.6 %
$t\bar{t}$	4347.08	3596.75	154.47	0.91	0.00556%
$t\bar{t}Z$	1.25	1.03	0.34	0.22	5.9 %

ratio \mathcal{R}' can be defined as

$$\mathcal{R}'(x_c) = \frac{1}{\sigma(\text{tot})} \int_0^{x_c} \frac{d\sigma}{dx'_\ell} dx'_\ell \equiv \frac{\sigma(x'_\ell \leq x_c)}{\sigma(\text{tot})}, \quad (8)$$

where $d\sigma/dx'_\ell$ is the differential cross section, and x'_c is the cut threshold of the energy fraction x'_ℓ .

We use a χ^2 -template method based on the W boson and top quark masses to select the three jets from the hadronic decay of the anti-top quark. For each event we pick the combination which minimizes the following χ^2 :

$$\chi^2 = \frac{(m_W - m_{jj})^2}{\Delta m_W^2} + \frac{(m_t - m_{jjj})^2}{\Delta m_t^2}, \quad (9)$$

where Δm_W and Δm_t are the width of the W -boson and the top quark, respectively. The efficiency of this method is 84%. After the antitop quark energy is reconstructed in the lab frame, \mathcal{R}' can be obtained with its cut threshold x'_c dependence.

Armed with both the Monte Carlo level momenta and the reconstructed momenta, we perform several comparisons to evaluate how faithful the \mathcal{R}' distribution is to the true \mathcal{R} . At the Monte Carlo level, t_{lep} and \bar{t}_{had} are known in the center-of-mass (cms) and lab frames. Our comparisons show that \mathcal{R} defined with t_{lep} is not sensitive to the boost from the cms to laboratory frame, whereas \mathcal{R} defined by \bar{t}_{had} shows a slight dependence. We compute the ratio \mathcal{R} defined from the energy of the t_{lep} and \bar{t}_{had} . At the detector simulation level, only the four-momentum of \bar{t}_{had} can be reconstructed, denoted $\bar{t}_{\text{had}}^{\text{rec}}$. Some of our results are compared in Fig. 2 (a) for choices $\sin \theta_{\text{eff}} = 1$ and $\cos \theta_{\text{eff}} = 1$ in Eq. 5. With $\sin \theta_{\text{eff}} = 1$ ($\cos \theta_{\text{eff}} = 1$) the top quark is mainly right-handed (left-handed), and we label the curves by t_R (t_L). There is some difference between the \mathcal{R} distributions for t_{lep} and \bar{t}_{had} , but the essential features are preserved. We conclude that x'_c is a good variable when x_c cannot be obtained. We also investigate the cut dependence of $\bar{t}_{\text{had}}^{\text{rec}}$ at the reconstruction level, whether basic or hard, and find that \mathcal{R} is not sensitive to the cuts; the curves for the loose cuts and the hard cuts overlap. Lastly, comparing \mathcal{R} at the Monte Carlo level and at the reconstruction level, we see a slight downward shift for both t_L and t_R . This effect arises because the p_T cuts on the lepton reduce the number of events with $x'_\ell < x'_c$.

The results in Fig. 2 (a) establish that x'_c is a suitable variable and that \mathcal{R}' serves as a good substitute for \mathcal{R} .

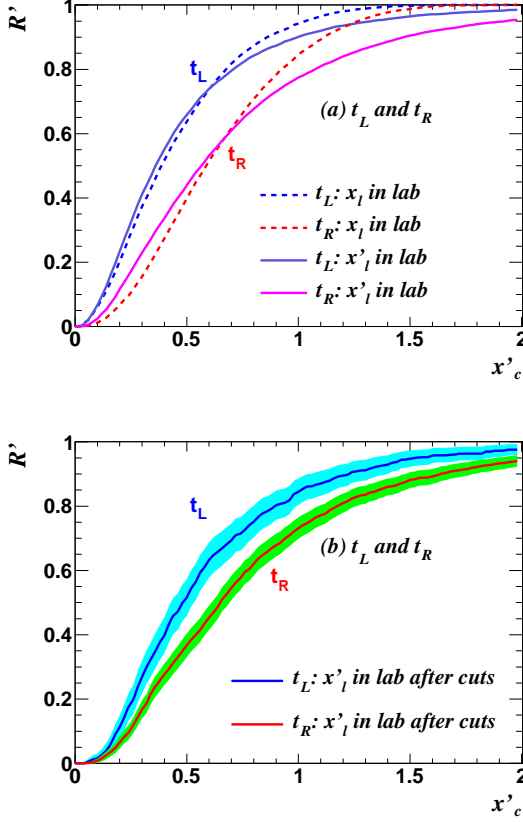


FIG. 2: (a) The \mathcal{R} distributions as a function of the cut threshold x'_c for a 350 GeV \tilde{t} quark with pure right-handed or left-handed couplings at the LHC with 8 TeV energy. The lepton energy fraction is evaluated in the lab frame from either $\tilde{t}_{\text{had}}^{\text{rec}}(x'_\ell)$ or the top quark energy $t_{\text{lep}}(x_\ell)$. (b) The statistical uncertainty band of \mathcal{R} is shown for both t_L and t_R at the 1σ confidence level for an assumed 20 fb^{-1} of integrated luminosity.

To show that the difference between the expectations for t_L and t_R can be observed, we include statistical uncertainties on the \mathcal{R} variable. Expressing

$$\mathcal{R}'(x'_c) = \frac{N(x'_\ell < x'_c)}{N(\text{tot})}, \quad (10)$$

where $N(\text{tot})$ is the total event number after cuts, and $N(x'_\ell < x'_c)$ ($N(x'_\ell > x'_c)$) represents events with $x'_\ell < x'_c$ ($x'_\ell > x'_c$), we derive the standard statistical uncertainty

$$\delta\sigma(x'_c) = \frac{1}{N(\text{tot})} \sqrt{\frac{N(x'_\ell < x'_c)N(x'_\ell > x'_c)}{N(\text{tot})}}. \quad (11)$$

The statistical uncertainties of the \mathcal{R} distributions for t_L and t_R are shown in Fig. 2 (b) at the 1σ confidence level with 20 fb^{-1} integrated luminosity. The distinction is evident between L and R . The t_L curve increases much faster than the t_R curve. The pattern of the distributions

of \mathcal{R} can be used to identify the top quark polarization. In order to distinguish t_L from an unpolarized top-quark, we define 10 bins in x'_c within the range (0.3, 1.3) and calculate χ^2 per degree-of-freedom (d.o.f) for the difference $\mathcal{R}'_L(x'_c) - \mathcal{R}'_0(x'_c)$:

$$\chi^2/\text{d.o.f} = \frac{1}{10} \sum_{i=1}^{10} \left(\frac{\mathcal{R}'_L(x'_c) - \mathcal{R}'_0(x'_c)}{\delta\sigma_L(x'_c)} \right)^2. \quad (12)$$

The subscript “0” denotes an unpolarized top-quark. The result for an unpolarized top-quark (t_0) is

$$\mathcal{R}'_0(x'_c) = (\mathcal{R}'_L(x'_c) + \mathcal{R}'_R(x'_c)) / 2. \quad (13)$$

After all the cuts, about 87 (101) signal events are needed to distinguish t_L (t_R) from t_0 at 95% confidence level (C.L.) in the absence of background, with only about 23 signal events to discriminate t_R from t_L .

Thus far in this section, we assume the $t\text{-}\tilde{t}\text{-}\tilde{\chi}$ coupling is completely left-handed or right-handed, but in general the coupling is a mixture of both. Once data are obtained, we could use the \mathcal{R}' curves shown in Fig. 2(b) as templates in fits to these data to extract θ_{eff} and shed light on the nature of top squark mixing.

Other implications: Our method can be applied to several NP models. We performed a detailed simulation of pair production of a T -odd top quark partner (T_-) in the Littlest Higgs Model with T -parity (LHT), $pp \rightarrow T_- \bar{T}_- X \rightarrow t \bar{t} A_H A_H X$, where A_H is the T -odd photon partner. Our numerical results are very similar to those shown for t_R in Fig. 2. Verification of mainly right-handed polarization would provide a powerful check of the model [11]. Another example is the leptophobic Z' boson, which couples only to the SM quarks. The top quark polarization could be used to probe the handedness of the $Z'\text{-}q\text{-}q$ coupling which is sensitive to how the SM quarks are gauged under the new gauge symmetry [12].

Acknowledgments The work by E.L.B. and H.Z. is supported in part by the U.S. DOE under Grant No. DE-AC02-06CH11357. H.Z. is also supported by DOE under the Grant No. DE-FG02-94ER40840. Q.H.C. is supported by the National Natural Science Foundation of China under Grant No. 11245003. J.H.Y. is supported by the U.S. National Science Foundation under Grant No. PHY-0855561.

-
- [1] G. Mahlon and S. J. Parke, Phys. Rev. D **53**, 4886 (1996) [hep-ph/9512264]; G. L. Kane, G. A. Ladinsky and C. P. Yuan, Phys. Rev. D **45**, 124 (1992).
 - [2] J. Cao, C. Han, L. Wu, J. M. Yang and Y. Zhang, arXiv:1206.3865; Y. Bai, H. -C. Cheng, J. Gallicchio and J. Gu, arXiv:1203.4813; X. -J. Bi, Q. -S. Yan and P. -F. Yin, Phys. Rev. D **85**, 035005 (2012); T. Plehn, M. Spannowsky and M. Takeuchi, JHEP **1208**, 091 (2012) [arXiv:1205.2696 [hep-ph]]; D. S. M. Alves,

- M. R. Buckley, P. J. Fox, J. D. Lykken and C. -T. Yu, arXiv:1205.5805 [hep-ph].
- [3] M. Perelstein and A. Weiler, JHEP **0903**, 141 (2009).
 - [4] A. Czarnecki, M. Jezabek and J. H. Kuhn, Nucl. Phys. B **351**, 70 (1991).
 - [5] C. R. Schmidt and M. E. Peskin, Phys. Rev. Lett. **69**, 410 (1992).
 - [6] H. Zhang, E. L. Berger, Q. -H. Cao, C. -R. Chen and G. Shaughnessy, Phys. Lett. B **696**, 68 (2011); E. L. Berger, Q. -H. Cao, C. -R. Chen, G. Shaughnessy and H. Zhang, Phys. Rev. Lett. **105**, 181802 (2010).
 - [7] J. Alwall, P. Demin, S. de Visscher, R. Frederix, M. Herquet, F. Maltoni, T. Plehn and D. L. Rainwater *et al.*, JHEP **0709**, 028 (2007).
 - [8] J. Pumplin, D. R. Stump, J. Huston, H. L. Lai, P. M. Nadolsky and W. K. Tung, JHEP **0207**, 012 (2002).
 - [9] T. Han, R. Mahbubani, D. G. E. Walker and L. -T. Wang, JHEP **0905**, 117 (2009).
 - [10] J. Shelton, Phys. Rev. D **79**, 014032 (2009).
 - [11] Q. -H. Cao, C. S. Li and C. -P. Yuan, Phys. Lett. B **668**, 24 (2008); M. M. Nojiri and M. Takeuchi, JHEP **0810**, 025 (2008).
 - [12] E. L. Berger, Q. -H. Cao, C. -R. Chen and H. Zhang, Phys. Rev. D **83**, 114026 (2011).
 - [13] Another useful variable in the literature is $E_\ell/(E_\ell + E_b)$ where the b -jet and ℓ^+ originate from the same top-quark decay [10].